JMEPEG (1994) 3:393-402

Review and Application of Closed-Loop Systems in Flow-Induced Corrosion

Z. Ahmed and Abdul Aleem B.J.

Various closed-loop systems have been developed in recent years to investigate flow-induced corrosion. Because of different parameters and techniques used by investigators, interpretation of results is often confusing and complicated. This paper presents a review of important techniques employed and interpretation of corrosion data.

Keywords

Reynolds number (Re), Schmidts number (Sc), Sherwood number (Sh), mass-transfer coefficient, limiting current density, diffusion coefficient, kinematic viscosity, pitting potential, protection potential, corrosion potential, open-circuit potential

1. Introduction

MASS transfer plays an important role in electrode kinetics. The transport processes determine the limiting current at which the concentration of the metal/electrolyte becomes zero, which corresponds to the maximum rate at which the electrode process can be carried out.

The effect of hydrodynamic flow on corrosion has been known for more than 50 years, but has lacked quantitative illustration. The understanding of corrosion mechanisms has been enhanced significantly over the past 20 years by the application of basic principles of mass and momentum transport. Because the nature of corrosion is electrochemical, electrochemical studies can be adapted and used to interpret, evaluate, and understand corrosion mechanisms.

The dependence of corrosion on velocity has been amply demonstrated, but little regard has been paid to the diffusional boundary layer. The dimensions of the diffusional layer are partly controlled by the Reynolds number (Re) and are also affected by properties contained in the Schmidt number (Sc). The Reynolds number describes hydrodynamic boundary-layer thickness as a function of velocity. The mass transfer at a solid/liquid interface can be determined by measuring the dissolution rate of the reaction. The hydrodynamic conditions that prevail close to the metal surface determine the magnitude of the mass transfer at the metal/electrolyte interface.

Flow-dependent corrosion has been studied extensively using a number of methods, such as rotating disk (Ref 1-5), rotating cylinder, coaxial cylinder, and tubular flow techniques. This paper will review the experimental methods that have been employed to study the effect of velocity on corrosion and will show how the hydrodynamic analysis can be applied to the study of corrosion and the electrochemical process. Results of work done on the corrosion of selected aluminum alloys in the Arabian Gulf are presented to illustrate how the results can be utilized to predict the corrosion behavior of material in flowing seawater.

Z. Ahmed and **Abdul Aleem B.J.**, Mechanical Engineering Department, King Fahd University of Petroleum & Minerals, Dhahran-31261, Saudi Arabia

2. Application of Nondimensional Parameters in Evaluation of Flow-Dependent Corrosion

Resistance to mass transfer is offered primarily by the hydrodynamics of the boundary layer. For instance, in the corrosion of steel, the flux of oxygen toward the metal surface is the controlling factor, whereas in the case of copper alloys the rate of corrosion is controlled by the diffusion of copper ions away from the surface. Thus, corrosion is directly proportional to the rate of mass transfer. A high rate of M^{z+} or OH^- transport may not allow the formation of a protective film.

Hydrodynamic mass-transfer considerations are handled by presenting corrosion rates in terms of dimensionless parameters. The number of variables occurring in mass-transfer problems is fairly large. They are combined in a suitable manner so that a few dimensionless variables are obtained; these are termed dimensionless groups. Two hydrodynamic parameters are important in establishing the mass-transfer effects on corrosion as a function of velocity:

$$\mathrm{Re} = \frac{Vd}{\nu} \qquad \text{(Eq 1)}$$

$$\mathrm{Sc} = \frac{\nu}{D} \qquad \text{(Eq 2)}$$

where V is velocity (m/s), d is the characteristic dimension of the corroding surface, ν is kinematic viscosity (m^2/s), and D is the diffusion coefficient of the reacting species. The Reynolds and Schmidt numbers give the velocity dependence of the limiting current under laminar and turbulent flow conditions.

The application of dimensional analysis and dimensionless groups in mass-transfer measurements has been found to be useful in obtaining quantitative information on flow-induced corrosion. Because the limiting current density is related to mass-transfer rate, electrochemical techniques are advantageous to the study of fluctuations in mass transfer.

Velocity is intimately related to limiting current density, the magnitude of which controls the corrosion rate and electro-

chemical parameters such as corrosion potential (E_{corr}), corrosion current (I_{corr}), and pitting potential (E_p) of alloys in flowing water. For a reaction that is diffusion controlled,

$$I_{lim} = KnF\Delta C \text{ or } K = \frac{I_{lim}}{nFC_b} \quad \text{(Eq 3)}$$

where I_{lim} is the limiting current density (A/cm^2), K is the mass-transfer coefficient (cm/s), n is the number of valence electrons involved, ΔC is the concentration driving form (mol/cm^3), F is Faraday's constant (Ampere – seconds/mole), and C_b is bulk concentration (mol/cm^3).

By measuring I_{lim} at a fixed ΔC, K can be determined. Similarly, if K is known, ΔC can be determined by measuring I_{lim}. If neither the anodic or the cathodic corrosion process is diffusion controlled, the rate of corrosion is given by:

$$I_{corr} = nF\Delta CK \quad \text{(Eq 4)}$$

The mass-transfer coefficient can be represented as a dimensionless Sherwood number (Sh). It can be calculated from I_{lim}:

$$Sh = \frac{Kd}{D} = \frac{I_{lim}}{nFC_bD} \quad \text{(Eq 5)}$$

where d is diameter (cm). The mass transfer at a liquid/solid interface is expressed commonly as a dimensionless power law:

$$\text{Corrosion Current, } I_{corr} = \eta F\Delta C \frac{D}{d} (RE)^a(SC)^b \quad \text{(Eq 6)}$$

The rates of corrosion can be predicted without testing if the other parameters are known. For a case of fully developed flow in a smooth tube, the most common correlation is:

$$Sh = 0.023\, Re^{0.8}\, Sc^{0.33} \quad \text{(Eq 7)}$$

By rearrangement of Eq 5 and substitution in Eq 7:

$$I_{lim} = 0.023\, nFv^{-0.47} D^{0.67} d_e^{-0.3} V^{0.9} C_b \quad \text{(Eq 8)}$$

The theoretical current density can be calculated from Eq 8 and compared with the experimental value to check for accuracy.

Electrochemical techniques can be used to measure mass-transfer rates and, implicitly, corrosion rates under specified conditions. K can be calculated from Eq 3 (as F and n are known), and ΔC can be measured at the outset of the experiment. One important disadvantage of using I_{lim} is the existence of a critical velocity above which the limiting current is not established. The information obtained from mass transfer can also be correlated with the current density required for cathodic protection of structures submerged in seawater (Ref 6). Knowledge of the Sherwood number and the limiting current density allows determination of the corrosion rate of a material under different flow conditions.

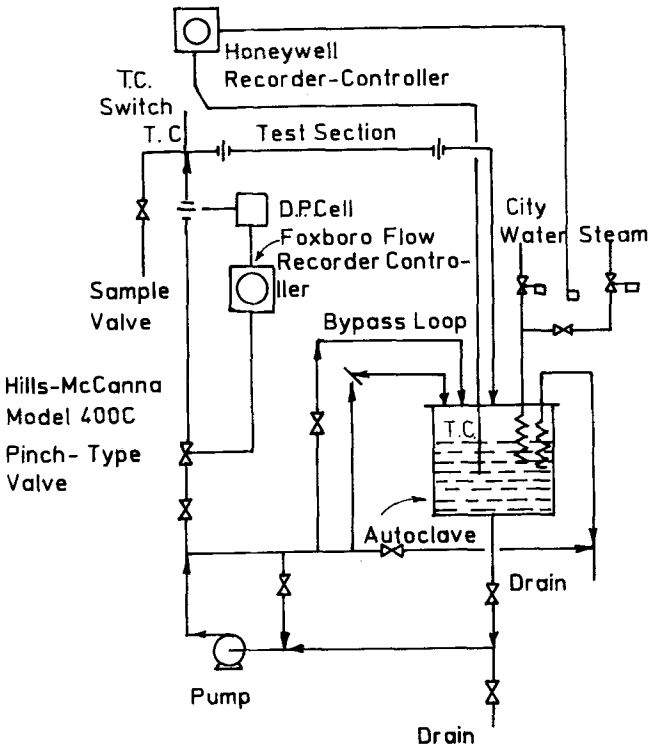

Fig. 1 Schematic diagram of a pipeline corrosion test apparatus

The understanding of corrosion mechanisms has been enhanced by the application of basic principles of mass transport. Mass-transport information obtained by the above experimental methods shows good correlation with corrosion rates determined using weight-loss and electrochemical techniques. Electrochemical techniques can be conveniently applied to determine the transport rates. The correlation of limiting current density with dimensionless groups has provided a strong tool for studying the effect of surface roughness, temperature, inhibitors, and several other parameters on the corrosion performance of materials.

3. Review of Closed-Loop Systems Developed to Study Flow-Induced Corrosion

A large number of closed-loop systems have been developed in recent years to study flow-induced corrosion. They are simple and convenient, and representative geometries can be tested in a consistent environment for a fixed period. Flow in pipes is the most frequently encountered geometry, and the system hydrodynamics is clearly defined. Hence, recirculating flow loops utilizing pipe specimens have been used often by investigators.

A schematic diagram of a pipeline corrosion test apparatus is shown in Fig. 1 (Ref 7). In the pipeline apparatus, corrosion rates were derived directly from weight-loss measurements over a definite period of time. Corrosion test specimens were short pieces of 25 mm (1 in.) pipe fitted between upstream and downstream runs of 25 mm (1 in.) pipe designed to ensure that

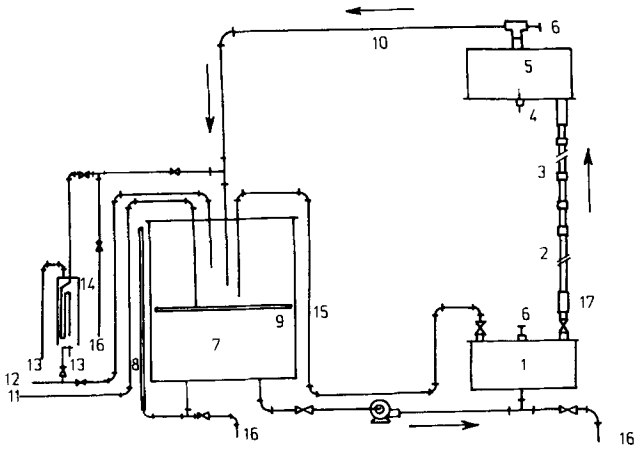

Fig. 2 Schematic diagram of a recirculating corrosion test apparatus. 1, distributor tank; 2, flow stabilizer; 3, test section; 4, Ag/AgCl electrode; 5, collecting tank; 6, thermometer; 7, supply tank; 8, level indicator; 9, air bubbler; 10, feedback line; 11, compressed-air line; 12, feedwater line; 13, sampling point; 14, sample cooler; 15, bypass line; 16, leading to drain; 17, flowmeter

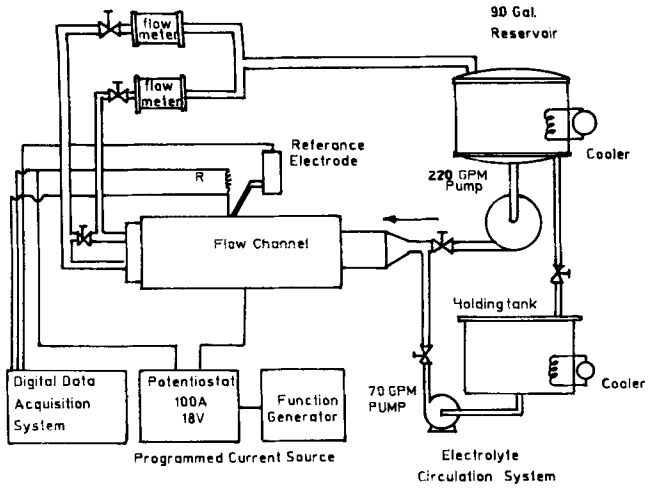

Fig. 3 Schematic diagram of an experimental system for measurement of limiting current density in a flow channel

fully developed flow conditions were maintained. The basic components of the test apparatus included the vessel, pump, flowmeters, test section, and control equipment. A temperature of 60 °C was maintained within ±2 °C. The data obtained from weight-loss studies were formulated into a Sherwood number.

Poulson (Ref 2) has described a test rig for making electrochemical measurements in flowing media. The test rig was constructed primarily from polyvinylidene fluoride (PVDF) material, chosen for its high chemical resistance. A PVDF centrifugal pump was used in the loop, and solution flow was measured by a rotameter. A provision in the loop was made for holding a variety of specimens, such as tubes, bends, and orifice specimens.

Another recirculating flow apparatus utilizing pipe specimens for corrosion studies is shown in Fig. 2 (Ref 8). It consisted of a heating tank, pump distributor, and collecting reservoir, along with the necessary valves and flowmeters. All components were fabricated from either polyethylene or neoprene—except for valves and pumps, which were lined with Heresite. The test sections were composed of 6 or 12 pieces of black iron pipe, 19 mm (0.75 in.) in diameter and 89 mm (3.5 in.) long. The technique used to determine corrosion rates involved measurement of specimen weight loss over a period of time for different flow rates, followed by visual and microscopic examination of corrosion products.

Another recirculating loop designed to measure the limiting current density of diffusion-controlled reactions is shown in Fig. 3 (Ref 9). In general, the limiting current density of diffusion-controlled cathodic reactions has been measured on inert electrodes. The most widely used redox systems for mass-transfer measurements are the ferro/ferricyanide, the iodide/iodine, and the copper/cupric ion systems. If the reactant is an ion, the contribution of the ionic migration to the mass transfer can be eliminated by using an excess of support electrolyte. Under such conditions the limiting current density is determined by diffusion through a laminar sublayer. The measuring cell used for the mass-transfer measurements consists of electrically isolated segmented electrodes. Cell packets with a varying number of electrodes and with a bored inner diameter ranging from 20 to 40 mm are manufactured from 10 mm nickel plate. To determine mass transfer, two flow cells with inner diameters of 20 and 40 mm, respectively, are used. Each flow cell consists of 27 electrodes 10 mm in length and two more electrodes 20 mm in length. The mass-transfer coefficient for an individual electrode is calculated by using mass-transfer correlations.

Studies involving measurements of corrosion rates under flow conditions have been reported by South (Ref 10). The corrosion rate in turbulent flowing hydrochloric acid at temperatures up to 80 °C has been determined using the polarization resistance method; the arrangement of the test rig is shown in Fig. 4.

A high-density polyvinyl chloride (PVC) loop has been recently developed by one of the authors to study the effects of several variables—including oxygen, pH, dissolved solids, chloride contents, suspended solids, and velocity—on the corrosion rates of various materials in seawater (Ref 11). This loop has proved very convenient for studying the effect of velocity on the corrosion resistance of tube and sheet materials. In general, all work related to the hydrodynamic testing of materials in seawater up to 65 °C can be performed using this equipment. The range of temperature can be increased if desired.

A schematic of the PVC test loop is shown in Fig. 5. The recirculating loop consists of entry and exit control valves, a manometer, a water pump, flowmeters, and differently sized holders that can accommodate several flat or tubular specimens. The diameter of each specimen holder is selected according to the velocity to which the specimens will be exposed. Water from a reservoir reaches the main system through an entry valve. A manometer is used to regulate the airflow in the system. The flow of water (aerated or deaerated) is similar in the three columns, each of which contains at least four specimen holders (although these can be increased or decreased as desired). Each specimen holder can accommodate up to six

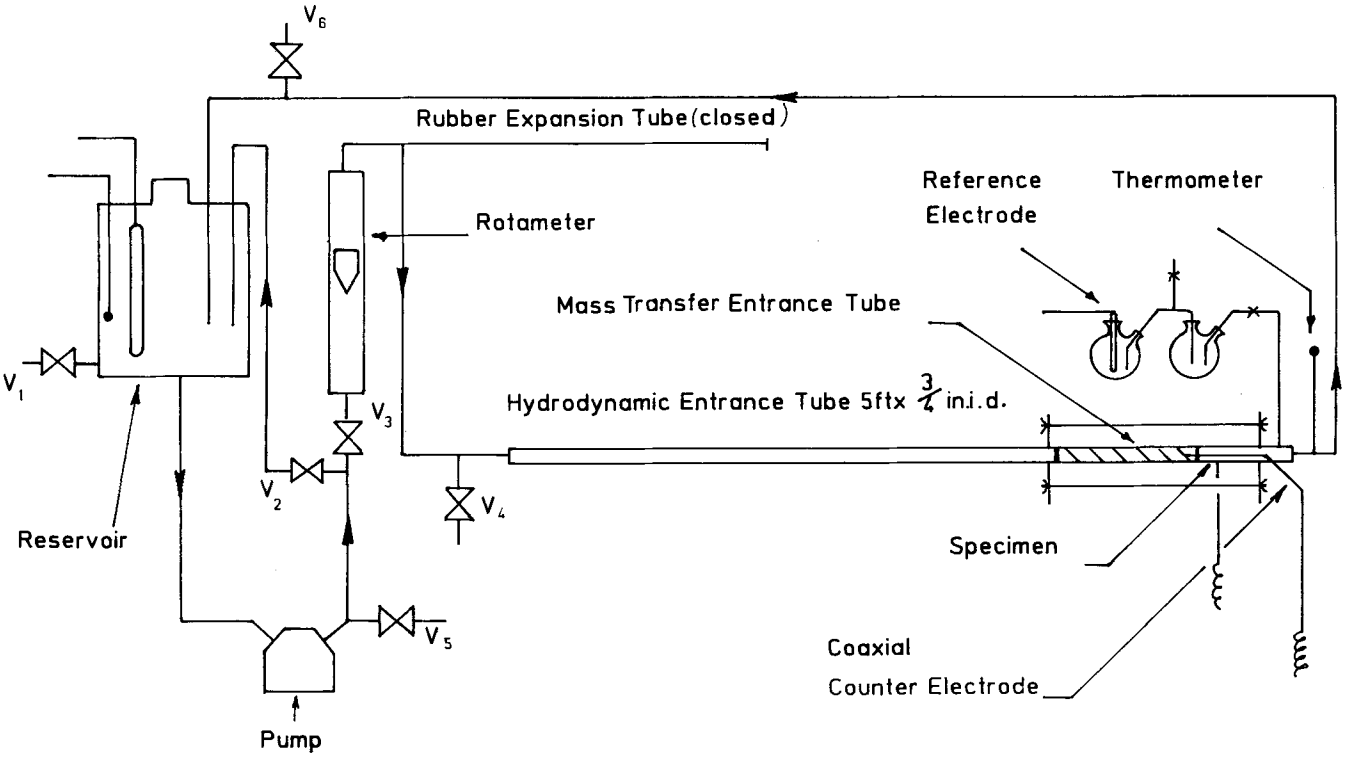

Fig. 4 Test rig for measuring corrosion rates under flow conditions

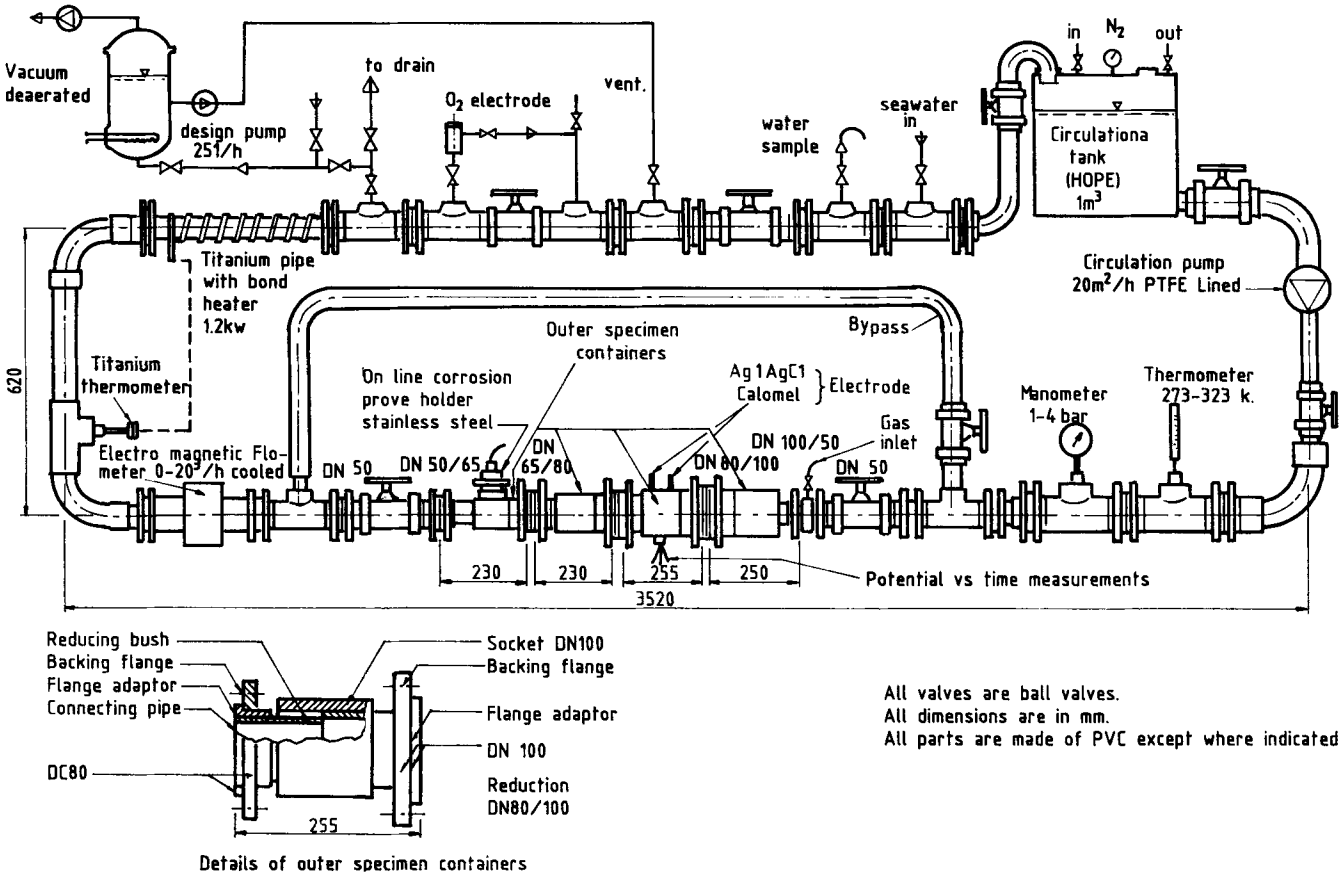

Fig. 5 Modified PVC loop for material testing under marine conditions

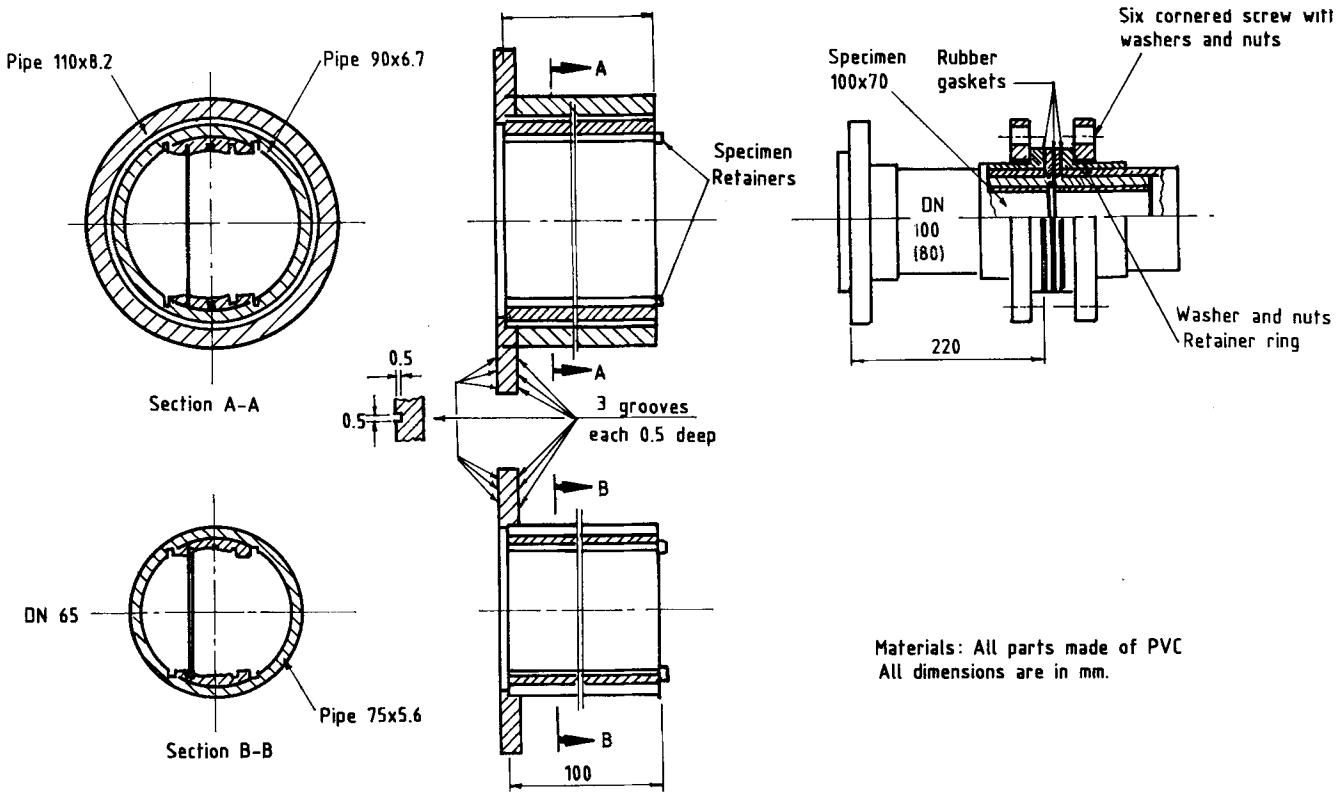

Fig. 6 Details of specimen containers shown in Fig. 5

specimens at once, and each holder is housed in an outside container. Details are shown in Fig. 6. Maximum velocity can be achieved by using a single column (one line) and minimum velocity by the use of all three lines. Also, the velocity can be varied by varying the diameters of the specimen holders or by varying the flow rate. Aeration is achieved by passing compressed air in the tank and deaeration by passing nitrogen. The pH is controlled by introducing a calculated amount of NaOH. This system allows convenient study of the effects of velocity changes in the bends and joints on corrosion.

4. Electrochemical Studies in Flow Loops

Flow in pipes is the most frequently encountered geometry, and the system hydrodynamics is clearly defined. Hence, recirculating flow loops and pipe specimens are often used by investigators. Electrochemical polarization measurements can be made in the flow loop by providing sufficient entry length preceding the specimens to allow the hydrodynamic boundary layer to be established. For Reynolds numbers between 100 and 1000, an entry length of 3.5 to 70*d* is required. For Reynolds numbers between 3000 and 100,000, an entry length of 5.2 to 123*d* is required. The reference electrode (standard calomel electrode, SCE), counterelectrode (graphite), and the specimens in the loop are connected to a potentiostat for obtaining different polarization curves. The polarization resistance, potentiodynamic, and Tafel plots are obtained in the loop in accordance with standard ASTM recommended practice (Ref 12).

A rotating-disk electrode assembly is employed to derive the mass-transfer coefficient by measuring the limiting current density. The number of revolutions is measured by a counter. The working potential is first determined by polarization curves and is set at this value in the potentiostat. Generally, the rotational speed is set at 100 rev/min and the potential allowed to stabilize. The rotational speed is then increased to the next higher setting, and cathodic polarization curves are recorded. The potential is impressed in the negative direction in small steps of 10 or 20 mV until the limiting current region is reached. Limiting current density is plotted as a function of the square root of the angular velocity (Ref 13). Anodic polarization curves can be recorded in a similar manner.

5. Interpretation and Analysis of Data Obtained from Recirculating-Loop and Electrochemical Measurements

A summary of work conducted on the flow-induced corrosion of a modified aluminum alloy in the flow loop described above (Ref 14) is presented here to show how the effect of velocity on corrosion resistance can be evaluated and interpreted.

5.1 *Material*

Flat specimens of modified aluminum alloy were used; the alloy composition is given in Table 1 (Ref 14). An analysis of the Arabian Gulf water in which the tests were conducted is given in Table 2.

5.2 *Specimen Preparation*

The samples were cleaned using a hot commercial detergent and rinsed with potable water. The samples were exposed to a solution of 20 g of $K_2Cr_2O_7$, 28 mL of phosphoric acid, and enough demineralized water to make 1 L at 70 to 80 °C; they were then degreased by washing in acetone, rinsing in demineralized water, and cleaning with an ultrasonic cleaner. The samples were dried overnight in a desiccator before being weighed. The corroded samples were treated with a phosphate/chromate mixture to remove corrosion products. For metallographic studies, 1.5 cm^2 samples were cut and mounted in Bakelite. They were polished on 600-grit silicon carbide tape and final polished with 0.5 μm alumina paste in distilled water. For scanning electron microscopy the samples were gold coated at 1200 V under a vacuum of 0.13 Pa (10^{-3} torr) for 5 min. The polished specimens were cleaned ultrasonically.

5.3 *Experimental Method*

The high-density PVC recirculating loop described above was used to investigate the effect of velocity. Electrochemical polarization studies were conducted in accordance with ASTM Standard Practice G 59. An EG & G model 616 rotating-disk assembly was used to determine limiting density (Ref 13). For polarization measurement, an EG & G potentiostat model 273 fitted with a microprocessor was used.

Table 1 Composition of the modified aluminum alloy

Element	Weight percent
Silicon	1.01
Iron	0.10
Copper	<0.01
Manganese	0.10
Magnesium	2.48
Chromium	0.22
Zinc	0.01
Titanium	0.003
Aluminum	bal

Table 2 Analysis of Arabian Gulf water

Ion	Content, mg/L
Na^+	19,186
Ca^{2+}	704
Mg^{2+}	2,400
SO_4^{2-}	4,894
Cl^-	34,080
CO_3^-	18
HCO_3^{2-}	189
Total	61,471

Table 3 Summary of weight-loss results in Arabian Gulf water in dynamic conditions

	Corrosion rate, mdd	
Reynolds number (Re)	Deaerated Arabian Gulf water	Aerated Arabian Gulf water
5.1×10^4	8.346	22.462
3.95×10^4	7.260	17.176
3.25×10^4	6.408	14.236
2.7×10^4	5.986	12.864

5.4 *Results*

The variation of corrosion rate with Reynolds numbers for the aluminum alloy in Arabian Gulf water is shown in Fig. 7 and Table 3. It is clear that the rate of corrosion increases as Reynolds number increases. The rate of corrosion, however, increases by only 2 mdd upon increasing the Reynolds number from 2.7×10^4 to 5.1×10^4. The overall increase in corrosion rate is thus very small and reflects the excellent corrosion resistance of the modified alloy in Arabian Gulf water. However, corrosion rate is very sensitive to changes in oxygen concentration. In aerated water (~5.3 ppm O_2, the rate of corrosion is almost doubled (~14 mdd) compared to deaerated seawater (~6 mdd) at $Re = 2.7 \times 10^4$. The total increase in the rate of corrosion observed in aerated seawater upon changing the Reynolds number from 2.7×10^4 to 5.1×10^4 is 10 mdd. The effect of oxygen is clearly apparent.

Oxygen reduces the corrosion of aluminum by forming a protective oxide film that serves as an effective barrier to further attack. On the other hand, oxygen also promotes corrosion through the depolarization of local cathodic areas by unblocking the cathodic reaction and enabling the environment to react further with the metal. It has been reported that low concentrations of oxygen are beneficial and that higher concentrations do not further alter the rate of corrosion (Ref 15). In deaerated seawater, the primary cathodic reaction is the reduction of solvent molecules to form molecular hydrogen. Aluminum corrodes very slowly and uniformly in deaerated seawater. However, on passing oxygen, the total cathodic current is increased:

$$2H^+ + 2e^- \rightarrow H_2 \text{ or } \tfrac{1}{2}O_2 + H_2O + 2e^- \rightarrow 2OH \qquad \text{(Eq 9)}$$

The reduction reaction is catalyzed and the corrosion rate of aluminum alloy is increased. In the Arabian Gulf water (pH

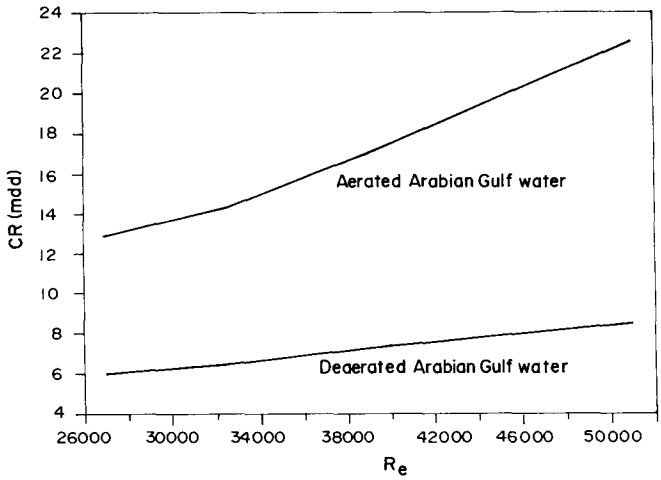

Fig. 7 Variation of corrosion rate with Reynolds number for a modified aluminum alloy in Arabian Gulf water

8.5), the transport of the hydroxide ion to the oxide solution interface controls the rate of reaction. At higher Reynolds numbers, the decreased thickness of the diffusion layer permits a greater flux of hydroxyl ions to interact with the electrode surface, and the corrosion rate increases. This accounts for the increase in the rate of corrosion of the modified aluminum alloy with increased Reynolds numbers.

6. Prediction of Corrosion Rate Utilizing Reynolds and Sherwood Numbers

By determining the Sherwood number experimentally, the relationship between the Sherwood number and the Reynolds number can be utilized to predict the magnitude of corrosion. Experimental values of Sherwood numbers for various Reynolds numbers are shown in Table 4. The Sherwood number increases linearly with the Reynolds number, suggesting that the rate of corrosion increases with increased Reynolds number (Fig. 8). The Sherwood number describes the maximum rate at which the hydroxyl ion is transported from the bulk solution to the metal surface. In the experimental determination of the Sherwood number, the following values were utilized:

$$\mathrm{Sh} = \frac{Kd}{D_o} = \frac{(\mathrm{C.R.[mdd]}(d))}{A(\Delta C)D} \qquad \text{(Eq 10)}$$

In Eq 10, A is the conversion factor between modes perquare centimeter-second and mdd. D_o was calculated from the relationship:

Table 4 Variation of Sherwood number with Reynolds number in Arabian Gulf water

Reynolds number (Re)	Sherwood number (Sh)
2.12×10^4	35.35
1.77×10^4	31.18
1.45×10^4	17.89
1.10×10^4	15.90

$$D_o^{0.67} = 1.61 \times I_{\mathrm{Lim}}\omega^{-6.5}\frac{\nu^{0.167}}{C_b ZF}$$

where

$$C_b = 0.25\times10^{-6}\ \mathrm{moles/cm^3}$$

$$I_{\mathrm{Lim}} = \left(\frac{i_{\mathrm{Lim}}}{S}\right)$$

i_{Lim} = limiting current = 15μA

S = surface area of electrode = 0.2 $\mathrm{cm^2}$

$\nu = 1.87\times10^{-2}\ \mathrm{cm^2/sec}$

$$\omega = 300\ \mathrm{rev/min} = \frac{300}{60}\times 2\pi = \frac{100\pi\ \mathrm{rad}}{\mathrm{s}}$$

7. Effect of Reynolds Number on Open-Circuit Potential

The variation of open-circuit potential (OCP) with Reynolds number is attributed to the formation and dissolution

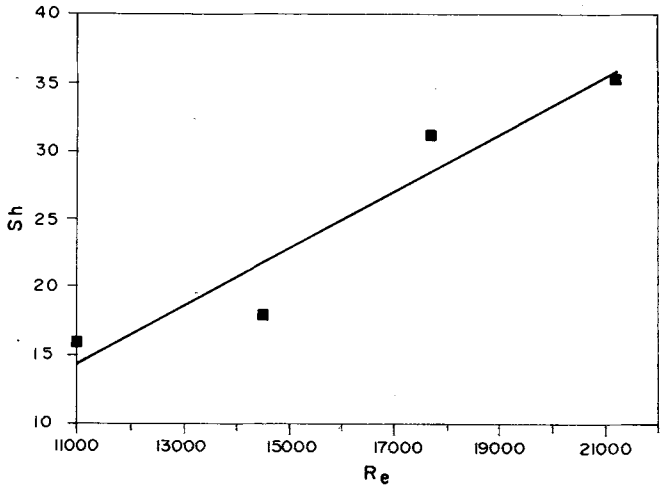

Fig. 8 Variation of Sherwood number with Reynolds number for a modified aluminum alloy in Arabian Gulf water

Table 5 Open-circuit potential characteristics of aluminum alloy in Arabian Gulf water

Reynolds number (Re)	Initial OCP, $\mathrm{mV_{SCE}}$	Final OCP, $\mathrm{mV_{SCE}}$	Difference in OCP, $\mathrm{mV_{SCE}}$	Time to reach equilibrium, h
1.1×10^4	−810.0	−858.0	−48.0	~160
1.45×10^4	−774.0	−827.0	−53.0	~160
1.77×10^4	−798.0	−843.0	−45.0	~170
2.12×10^4	−889.0	−965.0	−76.0	~190

Table 6 Values of E_p and E_{pp} obtained by potentiodynamic methods (dynamic conditions) in Arabian Gulf water

Reynolds number (Re)	Corrosion potential (E_{corr}), $\mathrm{mV_{SCE}}$	Pitting potential (E_p), $\mathrm{mV_{SCE}}$	Protection potential (E_{pp}), $\mathrm{mV_{SCE}}$	$\Delta E = E_p - E_{pp}$
2.12×10^4	−1113	−730	−835	105
1.77×10^4	−1146	−720	−821	101
1.45×10^4	−1201	−710	−808	98

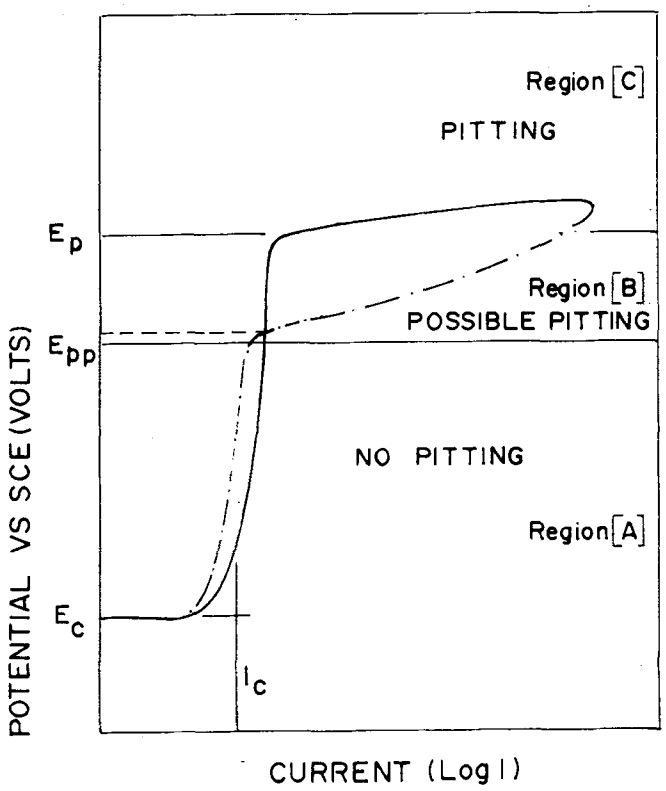

Fig. 9 Schematic diagram of a typical anodic polarization curve showing various regions of pitting

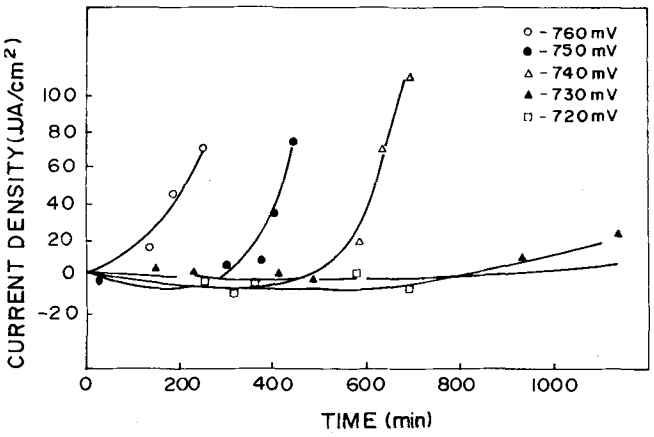

Fig. 10 Current-time diagram for a modified aluminum alloy in Arabian Gulf water

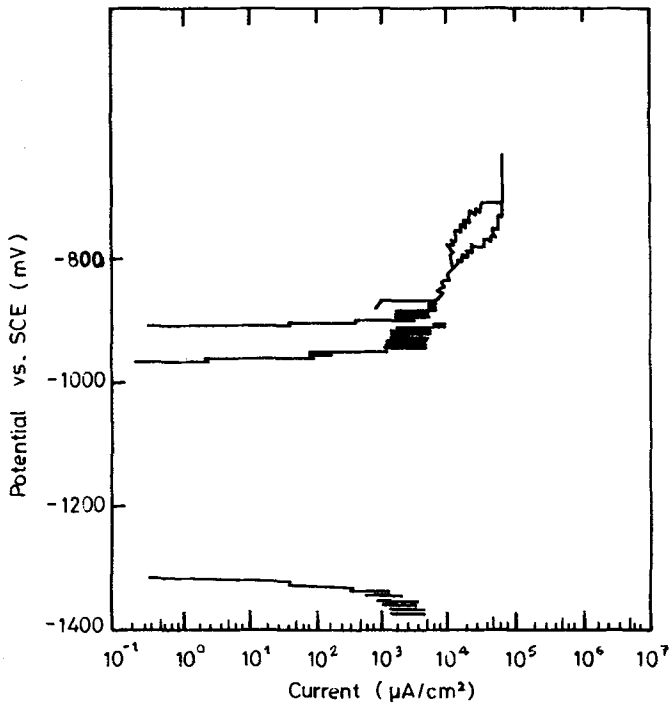

Fig. 11 Hysteresis loop for an aluminum alloy in Arabian Gulf water in a dynamic condition (velocity, 2.48 m/s)

of the protective oxide film formed on the aluminum alloy surface. The variation of OCP with Reynolds number is shown in Table 5. On increasing the Reynolds number from 1.1×10^4 to 2.12×10^4, the OCP shifts from –0.858 to –0.965 mV_{SCE}. An increase in potential in the positive direction (positive shift) indicates the formation of a protective film on the metal surface. A decrease in potential negative shift, on the other hand, indicates a change in the corrosion mechanism from anodic to cathodic control (from the release of Al^{3+} from the surface to the evolution of hydrogen [$2H^+ + 2e^- \rightarrow H^2$]). The decrease in potential also suggests decreasing anodic polarization and increasing polarization of the cathodic reduction (Ref 16). By observing the changes in OCP with time at different Reynolds numbers, the pitting tendency of aluminum alloys can be predicted. The alloy is not subjected to pitting if it remains in a range of potential close to the corrosion potential and below the pitting potential (E_p). Propagation of pits on aluminum alloy surfaces may continue even at potential sufficiently negative to E_p if the potential has at some stage shifted to a value close to the pitting potential.

8. Electrochemical Evaluation of Pitting Resistance

Polarization hysteresis curves have been used successfully to evaluate the pitting resistance of aluminum alloys (Ref 17). A typical polarization hysteresis curve is shown in Fig. 9. The curve is characterized by three well-defined regions: pitting initiation, pitting propagation, and no pitting. Pits initiate at a specific potential called pitting potential (E_p). The pitting potential is characterized by an abrupt increase in current density. The interaction of the reverse polarization curve with the forward anodic polarization curve yields the protection potential (E_p), which signifies the repassivation tendency of pits. Pits may propagate between E_p and E_{pp}, but new pits do not initiate in this region. Pitting is not expected between E_{corr} and E_{pp}.

Although the above criterion has been widely used for predicting the pitting susceptibility of aluminum alloys, it is criticized by some researchers. In particular, there is some disagreement about the existence of a protection potential (Ref

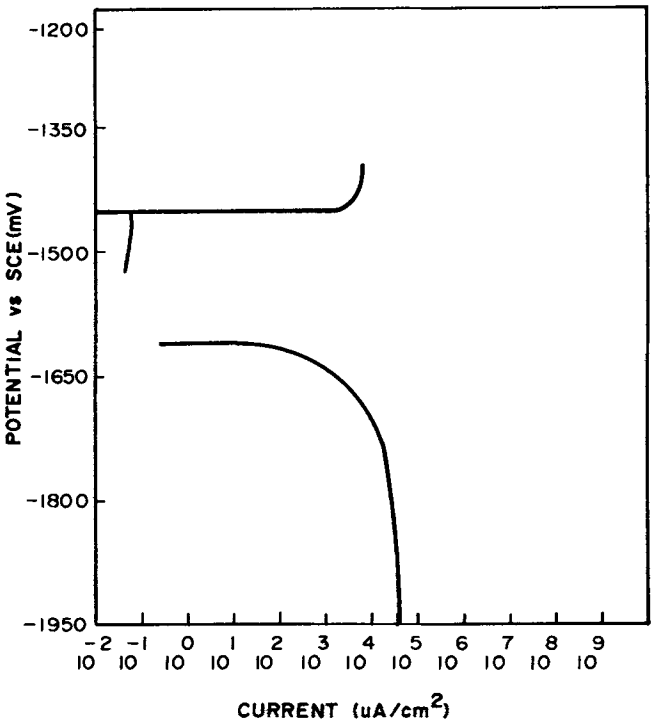

Fig. 12 Cathodic polarization curve for an aluminum alloy in Arabian Gulf water containing 2 vol% silica sand as suspended particles in a dynamic condition (velocity, 2.10 m/s)

18). However, qualitative prediction of the pitting susceptibility of aluminum alloys can be made with a certain degree of accuracy. More accurate values of pitting potential can be determined from curves obtained potentiostatically (Fig. 10). An increase in Reynolds number from 1.45×10^4 to 2.12×10^4 decreases the pitting potential from -710 to -730 mV_{SCE} (Table 6). The increased rate of mass transfer of OH^- shifts the pitting potential to more negative values, and pitting is observed at a lower value of potential (Fig. 11).

9. Application of Limiting Current Density

The limiting current density can be obtained experimentally by driving a cathodic reaction to a maximum rate until the limiting current is reached (Ref 19)—indicated by a current plateau on a current potential plot. When the limiting current is approached, the overpotential increases rapidly for every increment of current; however, a plateau is reached beyond which the current cannot flow.

As mentioned earlier, the limiting current density provides a convenient means for calculating the mass-transport coefficient, K. A cathodic polarization curve for an aluminum alloy showing limiting current density is illustrated in Fig. 12. An increase in the limiting current density suggests an increase in the corrosion rate. The limiting current density can be calculated theoretically by the relationship shown in Eq 8 and compared with experimental values of I_{lim} obtained potentiostatically. For instance, by inserting the following values for Al-2.5Mg alloy,

Table 7 Variation of corrosion rate in Arabian Gulf water with and without inhibitor addition

Reynolds number (Re)	Corrosion rate, mdd Without inhibitor	With inhibitor (50 ppm K_2CrO_4 + 50 ppm $NaHCO_3$)
2.12×10^4	16.040	5.85
1.45×10^4	10.662	4.86
1.1×10^4	8.285	3.98

$F = 96{,}487$ Ampere – seconds/mole
$\nu = 0.265 \times 10^{-2}$ cm^2/s
$D = 7.5 \times 10^{-3}$ cm^2/s
$d_e = 6.01$ cm
$V = 100$ cm/s
$O_2 = 10$ ppm

I_{lim} is calculated to be 10.7 μA/cm^2. The limiting current density can also be converted to the rate of corrosion in mils per year (mpy) or milligrams per square decimeter per day (mdd) by determining the correlation between mpy and current density (μA/cm^2):

$$1\ \mu A/cm^2 = 0.128 \left(\frac{\text{Atomic weight of element}}{\text{Valency} \times \text{density}} \right) \times \text{Percent of element in alloy} \quad \text{(Eq 11)}$$

For aluminum,

$$1\ \mu A/cm^2 = 0.4221\ \text{mpy}$$

It has been observed that I_{lim} increases with Reynolds number for both turbulent and laminar flow. If the corrosion potential (E_{corr}), pitting potential (E_p), or protection potential (E_{pp}) shifts in the positive direction, the anodic polarization remains largely unaffected by velocity, whereas a shift in the negative direction suggests that the anodic polarization is affected by velocity. Because of an increase in velocity, the cathodic process in aluminum alloy may shift from oxygen reduction to hydrogen evolution, the latter being activation controlled.

10. Corrosion Inhibition

The effectiveness of an inhibitor in flowing seawater can be investigated in the recirculating loop. For instance, the rate of corrosion at different Reynolds numbers decreased upon addition of 50 ppm K_2CrO_4 + 50 ppm $NaHCO_3$, as shown in Table 7.

11. Conclusions

- A recirculating-loop system allows investigation of the flow-induced corrosion of representative geometries under constant environments over a fixed period of time.
- By interfacing an electrochemical measurement system with the loop, parameters such as corrosion potential, pitting potential, and protection potential can be determined under different flow conditions.

- The rate of corrosion can be studied under laminar and turbulent flow conditions.
- A high-density PVC recirculating test loop interfaced with electrochemical devices can be used to evaluate corrosion hydrodynamics, as illustrated by the results of an investigation of a modified aluminum alloy in flowing Arabian Gulf water.

References

1. E. Heitz, G. Kreysa, and C. Loss, Investigation of Hydrodynamic Test Systems for the Selection of High Flow Rate Resistant Materials, *J. Appl. Chem.*, Vol 9, 1979, p 243-253
2. B. Poulson, Electrochemical Measurements in Flowing Solutions, *Corros. Sci.*, Vol 23 (No. 4), 1983, p 391-430
3. J. Postlethwaite, M.H. Dobbin, and K. Bergevin, The Role of Oxygen Mass Transfer in the Erosion of Slurry Pipelines, *Corrosion*, Vol 42 (No. 9), Sept 1986
4. B.T. Ellison and W.R. Schmeal, Corrosion of Steel in Concentrated Sulphuric Acid, *J. Electrochem. Soc.*, Vol 125 (No. 4), April 1978
5. V.G. Levich, *Physico Hydrodynamics*, Prentice Hall, 1962
6. W. Van Krevelen et al., *C.J. Rec. Trav. Chim, Pays-Bas*, Vol 66, 1947, p 5113
7. R.L. Cowan, Corrosion of Carbon Steel in Operating Desalting Plant, *Corrosion, 73* NACE conference, Anaheim, CA, March 1973
8. T.K. Ross and B.P.L. Hitchen, Some Effects of Electrolytic Motion during Corrosion, *Corros. Sci.*, Vol ?, 1986, p 67-75
9. T. Sydberger and U. Lotz, Relation between Mass Transfer and Corrosion in a Turbulent Pipe Flow, *J. Electrochem. Soc.*, Vol 129 (No. 2), 1982
10. K.D. South, "Electrochemical Measurements in Flowing Inhibited Acid," Master's thesis, Brunel University, London, 1969
11. Z. Ahmad, Effect of Velocity in Corrosion Behavior of Al-3Mg in North Sea Water, *Métaux-Corros.-Ind.*, Vol LV11 (No. 677), Jan 1982, p 11-26
12. *Annual Book of ASTM Standards*, Vol 203, ASTM, 1984
13. E. Heitz and G. Kreysa, *Principles of Electrochemistry Engineering*, Extended Version, VCH, 1986
14. Z. Ahmad, *Anti-Corrosion*, June 1981, p 4-7
15. P.F. George and S.V. Carleton, "Evaluation of Materials Performance After 18 Months Operation of the Aluminium Desalination Test Plant," 2nd Report, 31 March 1971
16. R.A. Bonewitz, An Electrochemical Evaluation of 1100, 5052 and 6063 Aluminium Alloy for Desalination, *Corrosion*, June 1971, p 215
17. A. Zaki and S. Rashidi, *Desalination*, Vol 44, 1983, p 265
18. J.A. Richardson and G.C. Wood, *Corros. Sci.*, Vol 10, 1970, p 315
19. A.C. Riddleford, The Rotating Disc System, *Advances in Electrochemistry and Electrochemical Engineering*, Vol 4, Interscience, 1965